


On Performance Modeling for MANETs Under General Limited Buffer Constraint

Jia Liu, *Member, IEEE*, Yang Xu, *Member, IEEE*, Yulong Shen, *Member, IEEE*, Xiaohong Jiang, *Senior Member, IEEE*, and Tarik Taleb , *Senior Member, IEEE*

Abstract—Understanding the real achievable performance of mobile ad hoc networks (MANETs) under practical network constraints is of great importance for their applications in future highly heterogeneous wireless network environments. This paper explores, for the first time, the performance modeling for MANETs under a general limited buffer constraint, where each network node maintains a limited source buffer of size B_s to store its locally generated packets and also a limited shared relay buffer of size B_r to store relay packets for other nodes. Based on the Queuing theory and birth-death chain theory, we first develop a general theoretical framework to fully depict the source/relay buffer occupancy process in such a MANET, which applies to any distributed MAC protocol and any mobility model that leads to the uniform distribution of nodes' locations in steady state. With the help of this framework, we then derive the exact expressions of several key network performance metrics, including achievable throughput, throughput capacity, and expected end-to-end delay. We further conduct case studies under two network scenarios and provide the corresponding theoretical/simulation results to demonstrate the application as well as the efficiency of our theoretical framework. Finally, we present extensive numerical results to illustrate the impacts of buffer constraint on the performance of a buffer-limited MANET.

Index Terms—Buffer constraint, delay, mobile ad hoc networks, performance modeling, throughput.

I. INTRODUCTION

THE mobile ad hoc networks (MANETs), a class of self-autonomous and flexible wireless networks, are highly appealing for lots of critical applications, like disaster relief,

battlefield communications, D2D communications for traffic offloading, and coverage extension in future 5G cellular networks [1]–[3]. In particular, the applications of MANETs in vehicle-to-vehicle communications, i.e., the vehicular ad hoc networks (VANETs) have attracted considerable academic attention recently as a promising solution to improving safety and driving experience [4], [5]. Motivated by these, understanding the fundamental performance limits of MANETs is of great importance to facilitate the application and commercialization of such networks [6], [7]. By now, extensive works have been devoted to the performance study of MANETs, which can be roughly classified into two categories, the ones with the consideration of practical limited buffer constraint and the ones without such consideration.

Regarding the performance study for MANETs without the buffer constraint, Grossglauser and Tse [8] first explored the capacity scaling law, i.e., how the per node throughput scales in the order sense as the number of network nodes increases, and demonstrated that with the help of node mobility a $\Theta(1)$ per node throughput is achievable in such networks. Later, Neely *et al.* [9] studied the delay-throughput tradeoff issue in a MANET under the independent and identically distributed (i.i.d) mobility model and showed that achievable delay-to-throughput ratio is lower bounded as $delay/throughput \geq O(n)$ (where n is the number of network nodes). Gamal *et al.* [10] then explored the delay-throughput tradeoff under a symmetric random walk mobility model, and showed that a $\Theta(n \log n)$ average packet delay is incurred to achieve the $\Theta(1)$ per node throughput there. Sharma *et al.* [11] further studied the delay-throughput tradeoff under a general and unified mobility model, and revealed that there exists a critical value of delay below which the node mobility is not helpful for capacity improvement. Recently, Wang *et al.* explored the throughput and delay performance for MANETs with multicast traffic in [12], [13], and further conducted the network performance comparison between the unicast and multicast MANETs in [14]. Those results indicate that the mobility can significantly decrease the multicast gain on per node capacity and delay, and thus weaken the distinction between the two traffic models.

While the above works represent a significant progress in the performance study of MANETs, in a practical MANET, however, the buffer size of a mobile node is usually limited due to both its storage limitation and computing limitation. Thus, understanding the real achievable performance of MANETs under the practical limited buffer constraint is of more importance for

Manuscript received November 12, 2016; revised April 3, 2017; accepted May 22, 2017. Date of publication May 31, 2017; date of current version October 13, 2017. This work was supported in part by the Project of Cyber Security Establishment with Inter-University Cooperation, in part by Secom Science and Technology Foundation, in part by Japan JSPS under Grant 15H02692, in part by China NSFC under Grants 61571352, 61373173, and U1536202, and in part by Research Foundation for Youths 20103176192. The review of this paper was coordinated by Y. Ji. (*Corresponding author: Yang Xu.*)

J. Liu is with the State Key Laboratory of Integrated Services Network, Xidian University, Xi'an 710071, China, and also with the Center for Cybersecurity Research and Development, National Institute of Informatics, Tokyo 101-8430, Japan (e-mail: jliu@nii.ac.jp).

Y. Xu is with the School of Economics and Management, Xidian University, Xi'an 710071, China (e-mail: yxu@xidian.edu.cn).

Y. Shen is with the State Key Laboratory of ISN, Xidian University, Xi'an 710071, China (e-mail: ylshen@mail.xidian.edu.cn).

X. Jiang is with the School of Systems Information Science, Future University Hakodate, Hakodate 041-8655, Japan (e-mail: jiang@fun.ac.jp).

T. Taleb is with the Sejong University, and also with Aalto University, Espoo 02150, Finland (e-mail: taleb-tarik@iee.org).

Digital Object Identifier 10.1109/TVT.2017.2710099

the design and performance optimization of such networks. By now, some initial results have been reported on the performance study of MANETs under buffer constraint [15]–[18]. Specifically, Herdtner and Chong [15] explored the throughput-storage tradeoff in MANETs and showed that the throughput capacity under the relay buffer constraint scales as $O(\sqrt{b/n})$ (where b is the relay buffer size of a node). Gao *et al.* [16] considered a MANET with limited source buffer in each node, and derived the corresponding cumulative distribution function of the source delay. Recently, the throughput and delay performance of MANETs are further explored under the scenarios where each node is equipped with an infinite source buffer and a shared limited relay buffer [17], [18].

A. Motivation

The motivation of our study is to take a step forward in the practical performance modeling for MANETs. In particular, this paper focuses on a practical MANET where each network node maintains a limited source buffer of size B_s to store its locally generated packets and also a limited shared relay buffer of size B_r to store relay packets for all other nodes. This buffer constraint is general in the sense that it covers all the buffer constraint assumptions adopted in available works as special cases, like the infinite buffer assumption [8]–[14] ($B_s \rightarrow \infty, B_r \rightarrow \infty$), limited source buffer assumption [16] ($0 \leq B_s < \infty, B_r \rightarrow \infty$), and limited relay buffer assumption [15], [17], [18] ($B_s \rightarrow \infty, 0 \leq B_r < \infty$). It should be pointed out that compared with the previous works [17], [18] where packet loss never occurs, under the general limited-buffer scenario packet loss is inevitable, which makes deriving achievable throughput a new challenging and significant problem, and the impacts of feedback mechanism on network performance worthy of study. To the best of our knowledge, this paper represents the first attempt on the exact performance modeling for MANETs under general limited-buffer constraint.

B. Our Contributions

The main contributions of this study are summarized as follows:

- 1) Based on the Queuing theory and birth-death chain theory, we first develop a general theoretical framework to fully depict the source/relay buffer occupancy process in a MANET with the general limited-buffer constraint, which applies to any distributed MAC protocol and any mobility model that leads to the uniform distribution of nodes' locations in steady state.
- 2) With the help of this framework, we then derive the exact expressions of several key network performance metrics, including achievable throughput, throughput capacity, and expected end-to-end (E2E) delay. We also provide the related theoretical analysis to reveal the fundamental network performance trend as the buffer size increases.
- 3) We further conduct case studies under two network scenarios and provide the corresponding theoretical/simulation results to demonstrate the efficiency and application of our theoretical framework. Finally, we present extensive

numerical results to illustrate the impacts of buffer constraint on network performance and our theoretical findings.

The remainder of this paper is organized as follows. Section II introduces the preliminaries involved in this paper. We analyze the buffer occupancy processes in Section III and derive the exact expressions for throughput, throughput capacity and expected E2E delay in Section IV. The case studies and simulation results are presented in Section V. The numerical results and corresponding discussions are provided in Section VI. Finally, we conclude this paper in Section VII.

II. PRELIMINARIES

In this section, we introduce the system models, the general limited buffer constraint, the routing scheme and performance metrics involved in this study.

A. System Models

Network Model: We consider a time-slotted MANET, which consists of n nodes randomly moving in a torus network area following a “uniform type” mobility model. With such mobility model, the location process of a node is stationary and ergodic with stationary distribution uniform on the network area, and the trajectories of different nodes are independent and identically distributed. It is notable that such “uniform type” mobility model covers many typical mobility models as special cases, like the i.i.d model [9], random walk model [10], and random direction model [19].

Traffic Model: We consider that there are n unicast traffic flows in the network, each node is the source of one traffic flow and also the destination of another traffic flow. More formally, let $\varphi(i)$ denote the destination node of the traffic flow originated from node i , then the source-destination pairs are matched in a way that the sequence $\{\varphi(1), \varphi(2), \dots, \varphi(n)\}$ is just a derangement of the set of nodes $\{1, 2, \dots, n\}$. This traffic model is widely adopted in other studies on the performance analysis of MANETs [8], [9], [11]. Two typical examples are $\varphi(1) = 2, \varphi(2) = 1, \varphi(3) = 4, \varphi(4) = 3, \dots, \varphi(n-1) = n, \varphi(n) = n-1$ (n is even), and $\varphi(1) = 2, \varphi(2) = 3, \dots, \varphi(n) = 1$. The packet generating process at each node is assumed to be a Bernoulli process with mean rate λ_s^+ , so that with probability λ_s^+ a new packet is generated in each time slot. During a time slot the total amount of data that can be transmitted from a transmitter to its corresponding receiver is fixed and normalized to one packet.

B. General Buffer Constraint

As illustrated in Fig. 1, we consider a general limited buffer constraint, where a node is equipped with a limited source buffer of size B_s and a limited relay buffer of size B_r . The source buffer is for storing the packets of its own flow (locally generated packets) and works as a FIFO (first-in-first-out) source queue [20], while the relay buffer is for storing packets of all other $n-2$ flows and works as $n-2$ FIFO virtual relay queues (one queue per flow). When a packet of other flows arrives and the relay buffer is not full, the corresponding relay

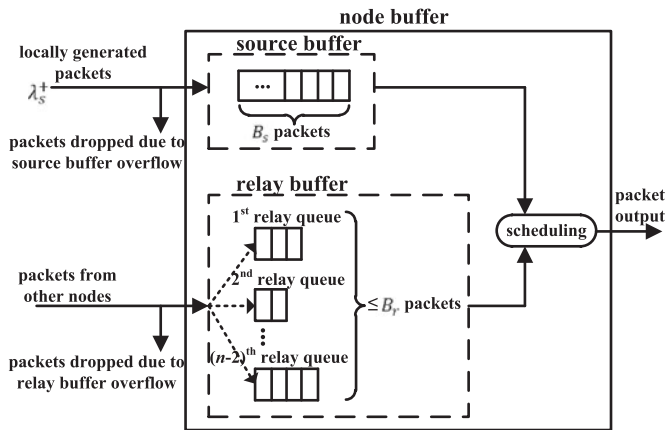


Fig. 1. Illustration of the general limited buffer constraint.

queue is dynamically allocated a buffer space; once a head-of-line (HoL) packet departs from its relay queue, this relay queue releases a buffer space to the common relay buffer. It is notable that the considered limited buffer constraint is general in the sense it covers all the buffer constraint assumptions adopted in the available works as special cases.

C. Two-Hop Relay Routing Without/With Feedback

Regarding the packet delivery scheme, we consider the two-hop relay (2HR) routing protocol. The 2HR scheme is simple yet efficient, and has been widely adopted in available studies on the performance modeling of MANETs [8], [9]. In addition to the conventional 2HR scheme without feedback, we also consider the 2HR scheme with feedback, which avoids packet loss caused by relay buffer overflow and thus can support the more efficient operation of buffer-limited MANETs.

Without loss of generality, we focus on a tagged flow and denote its source node and destination node as \mathcal{S} and \mathcal{D} respectively. Once \mathcal{S} gets access to wireless channel at the beginning of a time slot, it executes the 2HR scheme without/with feedback as follows.

1) (Source-to-Destination)

If \mathcal{D} is within the transmission range of \mathcal{S} , \mathcal{S} executes the Source-to-Destination operation. If the source queue of \mathcal{S} is not empty, \mathcal{S} transmits the HoL packet to \mathcal{D} ; else \mathcal{S} remains idle.

2) If \mathcal{D} is not within the transmission range of \mathcal{S} , \mathcal{S} randomly designates one of the nodes (say \mathcal{R}) within its transmission range as its receiver, and chooses one of the following two operations with equal probability.

a) (Source-to-Relay)

Without feedback: If the source queue of \mathcal{S} is not empty, \mathcal{S} transmits the HoL packet to \mathcal{R} ; else \mathcal{S} remains idle.

With feedback: \mathcal{R} sends a feedback to \mathcal{S} to indicate whether its relay buffer is full or not. If the relay buffer of \mathcal{R} is not full, \mathcal{S} executes the same operation as that without feedback; else \mathcal{S} remains idle.

b) (Relay-to-Destination)

In this operation, \mathcal{S} serves as the relay node forwarding packets to \mathcal{R} , and \mathcal{R} is the destination of packets forwarded from \mathcal{S} . If \mathcal{S} has packet(s) in the corresponding relay queue for \mathcal{R} , \mathcal{S} sends the HoL packet of this queue to \mathcal{R} ; else \mathcal{S} remains idle.

We let p_{sd} , p_{sr} and p_{rd} denote the probabilities that a node gets the chance to execute the Source-to-Destination, Source-to-Relay, and Relay-to-Destination operations, respectively.¹ It is worth noting that these probabilities are determined by the specific MANET scenario and will be regarded as known quantities in the following two sections, where the performance modeling is developed for a general MANET based on the basic system models mentioned above. The evaluations of p_{sd} , p_{sr} and p_{rd} will be shown in the case studies of Section V.

D. Performance Metrics

The performance metrics involved in this paper are defined as follows.

Throughput: The *throughput* T of a flow (in units of packets per slot) is defined as the time-average number of packets that can be delivered from its source to its destination.

Throughput Capacity: For the homogeneous finite buffer network scenario considered in this paper, the network level *throughput capacity* T_c can be defined by the maximal achievable per flow throughput, i.e., $T_c = \max_{\lambda_s^+ \in (0,1]} T$.

End-to-end Delay: The *end-to-end delay* D of a packet² (in units of slots) is defined as the time it takes the packet to reach its destination after it is generated by its source, and we use $\mathbb{E}\{D\}$ to denote the expectation of D .

III. BUFFER OCCUPANCY PROCESS ANALYSIS

In this section, we conduct the occupancy process analysis for both the source and relay buffers to determine their occupancy state distributions (OSDs), which will further help us to derive the exact expressions of the performance metrics T , T_c and $\mathbb{E}\{D\}$. Without loss of generality, we focus on a tagged node \mathcal{S} , and consider the scenarios without and with feedback, respectively.

A. OSDs Analysis Under the Scenario Without Feedback

1) *OSD of Source Buffer:* Regarding the source buffer of node \mathcal{S} , since in every time slot a new packet is generated with probability λ_s^+ and a service opportunity arises with probability μ_s being determined as

$$\mu_s = p_{sd} + p_{sr}, \quad (1)$$

the occupancy process of source buffer can be modeled by a B/B/1/ B_s queue as illustrated in Fig. 2.

Let $\pi_s(i)$ denote the probability that there are i packets occupying the source buffer in the stationary state, then the stationary

¹It should be noted that a node getting the chance to execute one operation in a time slot doesn't mean that it will conduct a transmission in this time slot.

²Notice that for the calculation of end-to-end delay, we only focus on the packets that have been successfully delivered to their destinations.

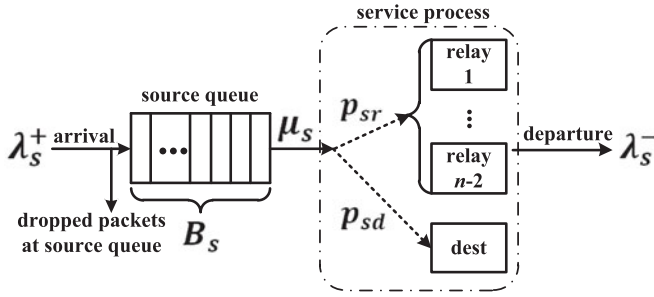


Fig. 2. Bernoulli/Bernoulli/1/ B_s queuing model for source buffer.

OSD of the source buffer $\Pi_s = [\pi_s(0), \pi_s(1), \dots, \pi_s(B_s)]$ can be determined as [21]

$$\pi_s(i) = \begin{cases} \frac{1}{1 - \lambda_s^+} H^{-1}, & i = 0 \\ \frac{1}{1 - \lambda_s^+} \frac{\tau^i}{1 - \mu_s} H^{-1}, & 1 \leq i \leq B_s \end{cases}$$

where

$$\tau = \frac{\lambda_s^+(1 - \mu_s)}{\mu_s(1 - \lambda_s^+)}, \quad (2)$$

and H is the normalization constant. Notice that $\Pi_s \cdot \mathbf{1} = 1$, where $\mathbf{1}$ is a column vector of size $(B_s + 1) \times 1$ with all elements being 1, we have

$$\pi_s(i) = \begin{cases} \frac{\mu_s - \lambda_s^+}{\mu_s - \lambda_s^+ \cdot \tau^{B_s}}, & i = 0 \\ \frac{\mu_s - \lambda_s^+}{\mu_s - \lambda_s^+ \cdot \tau^{B_s}} \frac{1}{1 - \mu_s} \tau^i. & 1 \leq i \leq B_s \end{cases} \quad (3)$$

2) *OSD of Relay Buffer*: We continue to analyze the occupancy process of the relay buffer in \mathcal{S} . Let X_t denote the number of packets in the relay buffer at time slot t , then the occupancy process of the relay buffer can be regarded as a stochastic process $\{X_t, t = 0, 1, 2, \dots\}$ on state space $\{0, 1, \dots, B_r\}$. Notice that when \mathcal{S} serves as a relay in a time slot, the Source-to-Relay transmission and Relay-to-Destination transmission will not happen simultaneously. Thus, suppose that the relay buffer is at state i in the current time slot, only one of the following transition scenarios may happen in the next time slot:

- 1) i to $i + 1$ ($0 \leq i \leq B_r - 1$): the relay buffer is not full, and a packet arrives at the relay buffer.
- 2) i to $i - 1$ ($1 \leq i \leq B_r$): the relay buffer is not empty, and a packet departs from the relay buffer.
- 3) i to i ($0 \leq i \leq B_r$): no packet arrives at and departs from the relay buffer.

Let $p_{i,j}$ denote the one-step transition probability from state i to state j ($0 \leq i, j \leq B_r$), then the occupancy process $\{X_t, t = 0, 1, 2, \dots\}$ can be modeled as a birth-death chain as illustrated in Fig. 3. Let $\pi_r(i)$ denote the probability that there are i packets occupying the relay buffer in the stationary state, the stationary OSD of the relay buffer $\Pi_r = [\pi_r(0), \pi_r(1), \dots, \pi_r(B_r)]$ is

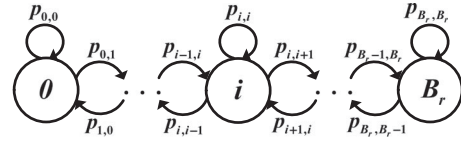


Fig. 3. State machine of the birth-death chain.

determined as

$$\Pi_r \cdot \mathbf{P} = \Pi_r, \quad (4)$$

$$\Pi_r \cdot \mathbf{1} = 1, \quad (5)$$

where \mathbf{P} is the one-step transition matrix of the birth-death chain defined as

$$\mathbf{P} = \begin{bmatrix} p_{0,0} & p_{0,1} & & & \\ p_{1,0} & p_{1,1} & p_{1,2} & & \\ & \ddots & \ddots & \ddots & \\ & & & p_{B_r-1,B_r-1} & p_{B_r-1,B_r} \end{bmatrix}, \quad (6)$$

and $\mathbf{1}$ is a column vector of size $(B_r + 1) \times 1$ with all elements being 1.

Notice that $p_{0,0} = 1 - p_{0,1}$, $p_{B_r,B_r} = 1 - p_{B_r,B_r-1}$ and $p_{i,i} = 1 - p_{i,i-1} - p_{i,i+1}$ for $0 < i < B_r$, the expressions (4)–(6) indicate that to derive Π_r , we need to determine the one-step transition probabilities $p_{i,i+1}$ and $p_{i,i-1}$.

Lemma 1: For the birth-death chain in Fig. 3, its one-step transition probabilities $p_{i,i+1}$ and $p_{i,i-1}$ are determined as

$$p_{i,i+1} = p_{sr} \cdot (1 - \pi_s(0)), \quad 0 \leq i \leq B_r - 1, \quad (7)$$

$$p_{i,i-1} = p_{rd} \cdot \frac{i}{n - 3 + i}, \quad 1 \leq i \leq B_r. \quad (8)$$

Proof: The proof is given in Appendix A. \blacksquare

By substituting (7) and (8) into (4) and (5), we can see that the stationary OSD of the relay buffer is determined as

$$\pi_r(i) = \frac{C_i (1 - \pi_s(0))^i}{\sum_{k=0}^{B_r} C_k (1 - \pi_s(0))^k}, \quad 0 \leq i \leq B_r \quad (9)$$

where $C_i = \binom{n-3+i}{i}$.

B. OSDs Analysis Under the Scenario With Feedback

Under the scenario with feedback, although node \mathcal{S} gets the chance to execute the Source-to-Relay operation in a time slot, it still remains idle if the relay buffer of its intended receiver is full (with the overflow probability $\pi_r(B_r)$), which causes the correlation between the OSD analysis of source buffer and that of relay buffer. It is notable, however, the overflow probability $\pi_r(B_r)$ only affects the service rate μ_s of the source buffer and the arrival rate at the relay buffer, while the occupancy processes of the source buffer and relay buffer can still be modeled as the B/B/1/ B_s queue and the birth-death chain respectively. Thus, based on the similar analysis as that in Section III-A, we have the following corollary.

Corollary 1: For the network scenario with feedback, the OSD Π_s of the source buffer and the OSD Π_r of the relay

buffer are determined as (3) and (9), where τ is given by (2), and the service rate μ_s of the source buffer is evaluated as

$$\mu_s = p_{sd} + p_{sr} \cdot (1 - \pi_r(B_r)). \quad (10)$$

Proof: The proof is given in Appendix B. ■

Corollary 1 indicates that for the evaluation of OSDs Π_s and Π_r , we need to determine the relay buffer overflow probability $\pi_r(B_r)$. From formula (9) we have

$$\pi_r(B_r) = \frac{C_{B_r} (1 - \pi_s(0))^{B_r}}{\sum_{k=0}^{B_r} C_k (1 - \pi_s(0))^k}, \quad (11)$$

where

$$\pi_s(0) = \frac{\mu_s - \lambda_s^+}{\mu_s - \lambda_s^+ \cdot \tau^{B_s}} = \frac{\mu_s - \lambda_s^+}{\mu_s - \lambda_s^+ \cdot \left(\frac{\lambda_s^+(1-\mu_s)}{\mu_s(1-\lambda_s^+)}\right)^{B_s}}. \quad (12)$$

We can see from (10)–(12) that (11) is actually an implicit function of $\pi_r(B_r)$, which can be solved by applying the fixed point theory [22]. We provide in Appendix C the detailed fixed point iteration for solving $\pi_r(B_r)$.

IV. PERFORMANCE ANALYSIS

With the help of OSDs of source buffer and relay buffer derived in Section III, this section focuses on the performance analysis of the concerned buffer limited MANET in terms of its throughput, expected E2E delay and throughput capacity.

A. Throughput and Expected E2E Delay

Regarding the throughput and expected E2E delay of a MANET with the general limited buffer constraint, we have the following theorem.

Theorem 1: For a concerned MANET with n nodes, packet generating rate λ_s^+ , source buffer size B_s and relay buffer size B_r , its per flow throughput T and expected E2E delay $\mathbb{E}\{D\}$ are given by

$$T = p_{sd} (1 - \pi_s(0)) + p_{sr} (1 - \pi_s(0)) (1 - \pi_r(B_r)), \quad (13)$$

$$\mathbb{E}\{D\} = \frac{1 + L_s}{\mu_s} + \frac{(n - 2 + L_r)(1 - \pi_r(B_r))}{p_{sd} + p_{sr}(1 - \pi_r(B_r))}, \quad (14)$$

where L_s (resp. L_r) denotes the expected number of packets in the source buffer (resp. relay buffer) under the condition that the source buffer (resp. relay buffer) is not full, which is determined as

$$L_s = \frac{\tau - B_s \tau^{B_s} + (B_s - 1) \tau^{B_s + 1}}{(1 - \tau)(1 - \tau^{B_s})}, \quad (15)$$

$$L_r = \frac{1}{1 - \pi_r(B_r)} \sum_{i=0}^{B_r - 1} i \pi_r(i), \quad (16)$$

μ_s is determined by (1) and (10) for the scenarios without and with feedback, respectively, τ , $\pi_s(0)$ and Π_r are determined by (2), (3) and (9), respectively.

Notice that packets of a flow are delivered to their destination through either one-hop transmission (Source-to-Destination) or two-hop transmission (Source-to-Relay and Relay-to-Destination), so the per flow throughput T can be derived by analyzing packet delivery rates of these two kinds of

transmissions. Regarding the expected E2E delay $\mathbb{E}\{D\}$, it can be evaluated based on the analysis of expected source queuing delay and expected delivery delay of a tagged packet.³ For the detailed proof of this theorem, please refer to Appendix D.

Remark 1: The formulas (13) and (14) hold for both network scenarios without/with feedback, but different network scenarios will lead to different results of τ , $\pi_s(0)$ and Π_r .

Based on the results of Theorem 1, we can establish the following corollary (See Appendix E for the proof).

Corollary 2: For a concerned MANET with the general limited buffer constraint, adopting the feedback mechanism improves its throughput performance.

B. Throughput Capacity and Limiting Throughput/Delay

To determine the throughput capacity T_c , we first need the following lemma (See Appendix F for the proof).

Lemma 2: For a concerned MANET with the general limited buffer constraint, its throughput T increases monotonically as the packet generating rate λ_s^+ increases.

Based on Lemma 2, we can establish the following theorem on throughput capacity.

Theorem 2: For a concerned MANET with n nodes, source buffer size B_s and relay buffer size B_r , its throughput capacity T_c is given by

$$T_c = p_{sd} + p_{sr} \frac{B_r}{n - 2 + B_r}. \quad (17)$$

Proof: Lemma 2 indicates that

$$T_c = \max_{\lambda_s^+ \in (0, 1]} T = \lim_{\lambda_s^+ \rightarrow 1} T. \quad (18)$$

From (2), (3) and (9) we can see that

$$\lim_{\lambda_s^+ \rightarrow 1} \tau = \lim_{\lambda_s^+ \rightarrow 1} \frac{\lambda_s^+(1 - \mu_s)}{\mu_s(1 - \lambda_s^+)} \rightarrow \infty, \quad (19)$$

$$\begin{aligned} \lim_{\lambda_s^+ \rightarrow 1} \pi_s(0) &= \lim_{\lambda_s^+ \rightarrow 1} \frac{\mu_s - \lambda_s^+}{\mu_s - \lambda_s^+ \cdot \tau^{B_s}} \\ &= \lim_{\tau \rightarrow \infty} \frac{\mu_s - 1}{\mu_s - \tau^{B_s}} = 0, \end{aligned} \quad (20)$$

$$\begin{aligned} \lim_{\lambda_s^+ \rightarrow 1} \pi_r(B_r) &= \lim_{\pi_s(0) \rightarrow 0} \frac{C_{B_r} (1 - \pi_s(0))^{B_r}}{\sum_{k=0}^{B_r} C_k (1 - \pi_s(0))^k} \\ &= \frac{C_{B_r}}{\sum_{k=0}^{B_r} C_k} = \frac{n - 2}{n - 2 + B_r}. \end{aligned} \quad (21)$$

Then T_c is given by

$$\begin{aligned} T_c &= \lim_{\lambda_s^+ \rightarrow 1} p_{sd} (1 - \pi_s(0)) + p_{sr} (1 - \pi_s(0)) (1 - \pi_r(B_r)) \\ &= p_{sd} \cdot (1 - 0) + p_{sr} \cdot (1 - 0) \cdot \left(1 - \frac{n - 2}{n - 2 + B_r}\right) \\ &= p_{sd} + p_{sr} \frac{B_r}{n - 2 + B_r}. \end{aligned}$$

³The source queuing delay of a packet is defined as the time it takes the packet to move to the HoL of its source queue after it is generated. The delivery delay of a packet is defined as the time it takes the packet to reach its destination after it moves to the HoL of its source queue.

Remark 2: We can see from Theorem 2 that the throughput capacity of the concerned MANET is the same for both the scenarios with and without feedback, and it is mainly determined by its relay buffer size B_r . We can further observe that when the network size n is extremely large while the relay buffer size B_r is fixed, the throughput is roughly equal to p_{sd} , which likes a unicast request only from a source node to its destination. This is because the service rate of a relay buffer is inversely proportional to the network size (please refer to Lemma 1) and thus will tend to 0 as n increases, indicating that packets can hardly be forwarded to their destinations through a relay node.

Based on Theorem 1 and Theorem 2, we have the following corollary regarding the limiting T and $\mathbb{E}\{D\}$ as the buffer size tends to infinity (See Appendix G for the proof).

Corollary 3: For a concerned MANET, its throughput increases as B_s and/or B_r increase. Moreover, as B_s and/or B_r tend to infinity, the corresponding limiting T and $\mathbb{E}\{D\}$ are determined as (22) and (23) respectively (shown at the bottom of this page), where $\rho_s = \min\{\frac{\lambda_s^+}{\mu_s}, 1\}$.

Remark 3: Corollary 3 indicates the throughput and delay results derived in Theorem 1 are universal in the sense that they cover the concise forms derived in other works as special cases. For example, they reduce to the results in [17], [18] as B_s tends to infinity, and the results in [9] as both B_s and B_r tend to infinity.

V. CASE STUDIES

In the previous two sections, with the basic probabilities p_{sd} , p_{sr} and p_{rd} , we have developed a theoretical framework for the performance modeling of a general MANET. These probabilities are determined by the specific MAC protocol adopted. To demonstrate the application and efficiency of our framework, in this section, we conduct case studies under network scenarios with two typical MAC protocols widely used in other studies concerning MANETs, and present corresponding theoretical/simulation results.

A. Network Scenarios

Cell-partitioned MANET with Local Scheduling based MAC (LS-MAC) [9], [11], [12], [23]: Under this network scenario, the whole network area is evenly partitioned into $m \times m$ non-overlapping cells. In each time slot one cell supports only one transmission between two nodes within it, and concurrent transmissions in different cells will not interfere with each other. When there are more than one node in a cell, each node in this cell becomes the transmitter equally likely. For such a MANET, the corresponding probabilities p_{sd} , p_{sr} and p_{rd} can be determined by the following formulas (See Appendix H for derivations).

$$p_{sd} = \frac{m^2}{n} - \frac{m^2 - 1}{n - 1} + \frac{m^2 - 1}{n(n - 1)} \left(1 - \frac{1}{m^2}\right)^{n-1}, \quad (24)$$

$$p_{sr} = p_{rd} = \frac{1}{2} \left\{ \frac{m^2 - 1}{n - 1} - \frac{m^2}{n - 1} \left(1 - \frac{1}{m^2}\right)^n - \left(1 - \frac{1}{m^2}\right)^{n-1} \right\}. \quad (25)$$

Cell-partitioned MANET with Equivalence Class based MAC (EC-MAC) [15], [24]–[26]: In such a MANET, the whole network area is evenly partitioned into $m \times m$ non-overlapping cells, and each transmitter (like the TX in Fig. 4(a)) has a transmission range that covers a set of cells with horizontal and vertical distance of no more than $\nu - 1$ cells away from the cell the transmitter resides in. To prevent simultaneous transmissions from interfering with each other, the EC-MAC is adopted. As illustrated in Fig. 4(b) that with the EC-MAC, all cells are divided into different ECs, and any two cells in the same EC have a horizontal and vertical distance of some multiple of ε cells. Each EC alternatively becomes active every ε^2 time slots, and each active cell of an active EC allows only one node in it (if any) to conduct data transmission. When there are more than one node in an active cell, each node in this cell becomes the transmitter equally likely. To enable as many number of

$$T = \begin{cases} p_{sd} \cdot \rho_s + p_{sr} \cdot \frac{\sum_{k=0}^{B_r-1} C_k \rho_s^{k+1}}{\sum_{k=0}^{B_r} C_k \rho_s^k}, & B_s \rightarrow \infty \\ (p_{sd} + p_{sr})(1 - \pi_s(0)), & B_r \rightarrow \infty \\ \min\{\lambda_s^+, p_{sd} + p_{sr}\}. & B_s \rightarrow \infty \text{ and } B_r \rightarrow \infty. \end{cases} \quad (22a)$$

$$T = \begin{cases} (p_{sd} + p_{sr})(1 - \pi_s(0)), & B_r \rightarrow \infty \end{cases} \quad (22b)$$

$$T = \begin{cases} \min\{\lambda_s^+, p_{sd} + p_{sr}\}. & B_s \rightarrow \infty \text{ and } B_r \rightarrow \infty. \end{cases} \quad (22c)$$

$$\mathbb{E}\{D\} = \begin{cases} \infty, & B_s \rightarrow \infty \text{ and } \lambda_s^+ \geq \mu_s \end{cases} \quad (23a)$$

$$\mathbb{E}\{D\} = \begin{cases} \frac{1 - \lambda_s^+}{\mu_s - \lambda_s^+} + \frac{(n - 2 + L_r)(1 - \pi_r(B_r))}{p_{sd} + p_{sr}(1 - \pi_r(B_r))}, & B_s \rightarrow \infty \text{ and } \lambda_s^+ < \mu_s \end{cases} \quad (23b)$$

$$\mathbb{E}\{D\} = \begin{cases} \frac{n - 2 + \pi_s(0) \cdot (1 + L_s)}{\pi_s(0) \cdot (p_{sd} + p_{sr})}, & B_r \rightarrow \infty \end{cases} \quad (23c)$$

$$\mathbb{E}\{D\} = \begin{cases} \frac{n - 1 - \lambda_s^+}{p_{sd} + p_{sr} - \lambda_s^+}, & B_s \rightarrow \infty, B_r \rightarrow \infty \text{ and } \lambda_s^+ < \mu_s. \end{cases} \quad (23d)$$

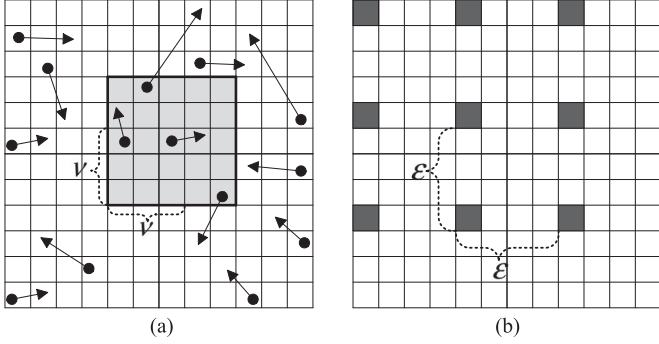


Fig. 4. A cell-partitioned MANET with EC-MAC. (a) Transmission range of a node. (b) Illustration of an EC (all the cells with gray color belong to the same EC).

concurrent transmissions to be scheduled as possible while avoiding interference among these transmissions, ε should be set as [17]

$$\varepsilon = \min\{\lceil(1 + \Delta)\sqrt{2\nu} + \nu\rceil, m\}, \quad (26)$$

where Δ is a guard factor specified by the protocol model [27].

For such a MANET, the corresponding probabilities p_{sd} , p_{sr} and p_{rd} are determined by the following formulas (See Appendix H for derivations).

$$p_{sd} = \frac{1}{\varepsilon^2} \left\{ \frac{\Gamma - \frac{m^2}{n}}{n-1} + \frac{m^2 - 1 - (\Gamma - 1)n}{n(n-1)} \left(1 - \frac{1}{m^2}\right)^{n-1} \right\}, \quad (27)$$

$$p_{sr} = p_{rd}$$

$$= \frac{1}{2\varepsilon^2} \left\{ \frac{m^2 - \Gamma}{n-1} \left(1 - \left(1 - \frac{1}{m^2}\right)^{n-1}\right) - \left(1 - \frac{\Gamma}{m^2}\right)^{n-1} \right\}, \quad (28)$$

where $\Gamma = (2\nu - 1)^2$.

By substituting the results of (24)-(25) and (26)-(28) into our theoretical framework, the network performance of a cell-partitioned MANET with LS-MAC and EC-MAC can be obtained, respectively. Our framework can easily apply to any other MAC protocol. For example, p_{sd} , p_{sr} and p_{rd} were derived for MANETs with Aloha protocol in [28], then the performance modeling of Aloha MANETs under the general limited buffer constraint can be accordingly conducted.

B. Simulation Settings

To validate our theoretical framework for MANET performance modeling, a simulator was developed to simulate the packet generating, packet queuing and packet delivery processes under above two network scenarios [29]. Each simulation task runs over a period of 2×10^8 time slots, and we only collect data from the last 80% of time slots to ensure the system is in the steady state. In the simulator, the following two typical mobility models have been implemented:

- 1) *I.i.d Model* [9]: At the beginning of each time slot, each node independently selects a cell among all cells with equal probability and then stays in it during this time slot.

- 2) *Random Walk (RW) Model* [10]: At the beginning of each time slot, each node independently selects a cell among its current cell and its 8 adjacent cells with equal probability $1/9$ and then stays in it during this time slot.

The detailed settings of network parameters in our simulations are summarized in Table I. Readers can also flexibly perform our C++ simulator with any other desired parameter settings.

C. Theoretical/Simulation Results

We summarize in Fig. 5 the theoretical/simulation results for throughput and delay under the above two network scenarios. For each scenario we consider the network settings of ($n = 72, m = 6, B_s = 5, B_r = 5$), and for the scenario with the EC-MAC protocol we set $\nu = 1$ and $\Delta = 1$ there [30]. Notice that the theoretical results here are obtained by substituting (24) and (25) (resp. (27) and (28)) into the formulas in Theorem 1.

Fig. 5 shows clearly that the simulation results match well with the theoretical ones for all the cases considered here, which indicates that our theoretical framework is applicable to and highly efficient for the performance modeling of different buffer limited MANETs. We can see from Fig. 5(a) and (c) that for a MANET with LS-MAC or EC-MAC, as the packet generating rate λ_s^+ increases, the per flow throughput T increases monotonically and finally converges to its throughput capacity T_c , which agrees with the conclusions of Lemma 2 and Theorem 2. Another interesting observation of Fig. 5(a) and (c) is that just as predicated by Corollary 2 and Theorem 2, although adopting the feedback mechanism usually leads to a higher throughput, it does not improve the throughput capacity performance.

Regarding the delay performance, we can see from Fig. 5(b) and (d) that in a MANET with either LS-MAC or EC-MAC, the behavior of expected E2E delay $\mathbb{E}\{D\}$ under the scenario without feedback is quite different from that under the scenario with feedback. As λ_s^+ increases, in the scenario without feedback $\mathbb{E}\{D\}$ first slightly increases and then decreases monotonically, while in the scenario with feedback $\mathbb{E}\{D\}$ first slightly increases, then decreases somewhat and finally increases monotonically. This is due to the reason that $\mathbb{E}\{D\}$ consists of source queuing delay and delivery delay, and the effects of λ_s^+ on $\mathbb{E}\{D\}$ are two folds. On one hand, a larger λ_s^+ leads to a more congested network with a larger $\pi_r(B_r)$ and a smaller μ_s (see formula (10)), which further leads to a larger expected source queuing delay; on the other hand, a larger $\pi_r(B_r)$ indicates that a packet is more likely to be delivered through a direct Source-to-Destination transmission, which further leads to a smaller expected delivery delay. As λ_s^+ increases, either of the two effects becomes dominant alternatively, causing the increase-decrease-increase phenomena of $\mathbb{E}\{D\}$ (it can be also seen in Fig. 7(b) and (d) later).

Moreover, the results in Fig. 5 indicate that although adopting the feedback mechanism leads to an improvement in per flow throughput, such improvement usually comes with a cost of a larger E2E delay. This is because that the feedback mechanism can avoid the packet dropping at a relay node, which contributes to the throughput improvement but at the same time makes the

TABLE I
SIMULATION SETTINGS

Parameters	n	m	B_s	B_r	ν	Δ	time slots	media access control	mobility model
Settings	72	6	5	5	1	1	2×10^8	LS-MAC and EC-MAC	i.i.d model and RW model

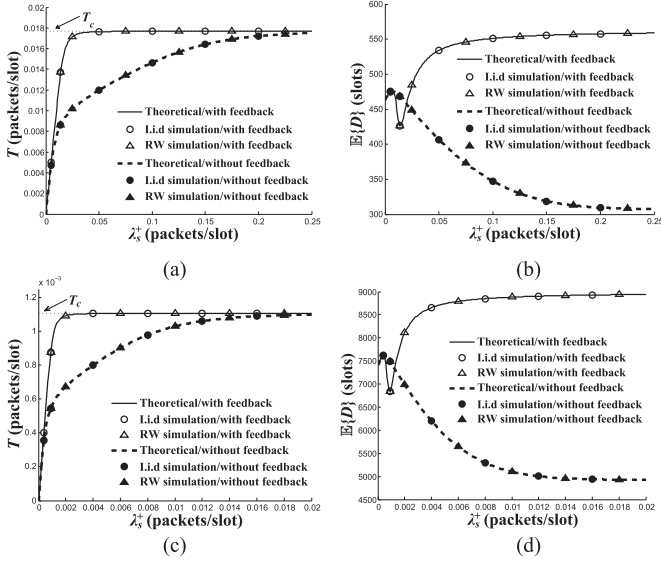


Fig. 5. Performance validation. (a) LS-MAC: T versus λ_s^+ . (b) LS-MAC: $\mathbb{E}\{D\}$ versus λ_s^+ . (c) EC-MAC: T versus λ_s^+ . (d) EC-MAC: $\mathbb{E}\{D\}$ versus λ_s^+ .

source/relay buffers tend to be more congested, leading to an increase in delay.

VI. NUMERICAL RESULTS AND DISCUSSIONS

Based on the proposed theoretical framework, this section presents extensive numerical results to illustrate the potential impacts of buffer constraint on network performance. Notice from Section V-C that the performance behaviors of the LS-MAC are quite similar to that of the EC-MAC, in the following discussions we only focus on a MANET with the LS-MAC.

We first summarize in Fig. 6 how T and $\mathbb{E}\{D\}$ vary with B_s and B_r under the settings of ($n = 72, m = 6, \lambda_s^+ = 0.05$). About the throughput performance, we can see from Fig. 6(a) and (c) that just as predicated by Corollary 3 and Corollary 2, T increases as either B_s or B_r increases, and the feedback mechanism can lead to an improvement in T . It is interesting to see that as B_s increases, T under the two scenarios without and with feedback converges to two distinct constants determined by (22a). As B_r increases, however, T under the two scenarios finally converges to the same constant determined by (22b).

Regarding the delay performance, Fig. 6(b) shows that as B_s increases, $\mathbb{E}\{D\}$ under the scenario without feedback quickly converges to a constant determined by (23b), while $\mathbb{E}\{D\}$ under the scenario with feedback monotonically increases to infinity, which agrees with the result of (23a). We can see from Fig. 6(d) that with the increase of B_r , however, $\mathbb{E}\{D\}$ under the scenario without feedback monotonically increases, while $\mathbb{E}\{D\}$ under the scenario with feedback first decreases and then increases.

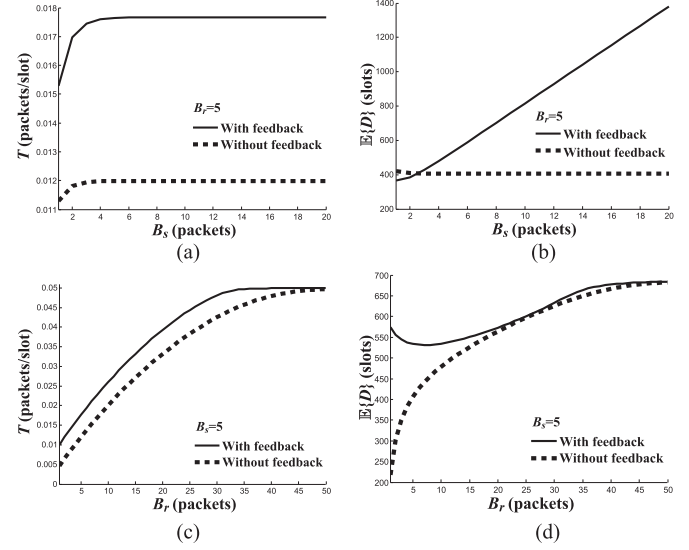


Fig. 6. Throughput and delay versus B_s and B_r for the network setting of ($n = 72, m = 6, \lambda_s^+ = 0.05$). (a) T versus B_s . (b) $\mathbb{E}\{D\}$ versus B_s . (c) T versus B_r . (d) $\mathbb{E}\{D\}$ versus B_r .

This is due to the reason that the effects of B_r on $\mathbb{E}\{D\}$ are also two folds. On one hand, a larger B_r leads to a less congested network with a smaller $\pi_r(B_r)$ and a larger μ_s , which further leads to a smaller expected source queuing delay; on the other hand, a larger B_r indicates that a packet is more likely to be delivered through a two-hop way (Source-to-Relay and Relay-to-Destination), which leads to a larger expected delivery delay. Similar to the throughput behavior in Fig. 6(c), (d) shows that as B_r increases $\mathbb{E}\{D\}$ under the two scenarios also converges to the same constant determined by (23c).

The results in Fig. 6 indicate that B_s and B_r have different impacts on the network performance in terms of T and $\mathbb{E}\{D\}$. In particular, as B_s increases, a notable performance gap between the scenarios without and with feedback always exist, where the throughput gap converges to a constant but the corresponding delay gap tends to infinity. As B_r increases, however, the performance gap between the two scenarios tends to decrease to 0, which implies that the benefits of adopting the feedback mechanism are diminishing in MANETs with a large relay buffer size. A further careful observation of Fig. 6 indicates that although we can improve the throughput by increasing B_s or B_r , it is more efficient to adopt a large B_r rather than a large B_s for such improvement. For example, under the scenario without feedback, Fig. 6(a) shows that by increasing B_s from 1 to 20, T can be improved from 0.0113 to 0.0120 (with an improvement of 6.19%); while Fig. 6(c) shows that by increasing B_r from 1 to 20, T can be improved from 0.0046 to 0.0332 (with an improvement of 621.74%).

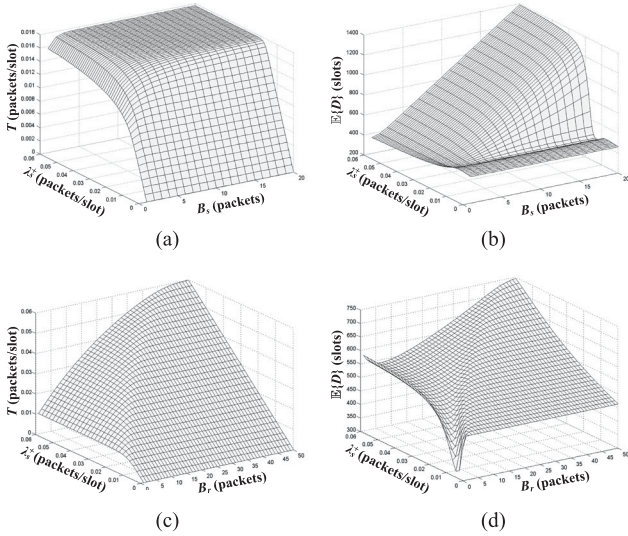


Fig. 7. Throughput and delay versus (λ_s^+, B_s) and (λ_s^+, B_r) for the network setting of $(n = 72, m = 6)$. (a) T versus (λ_s^+, B_s) , $B_r = 5$. (b) $\mathbb{E}\{D\}$ versus (λ_s^+, B_s) , $B_r = 5$. (c) T versus (λ_s^+, B_r) , $B_s = 5$. (d) $\mathbb{E}\{D\}$ versus (λ_s^+, B_r) , $B_s = 5$.

To further illustrate how the impacts of buffer size on network performance are dependent on packet generating rate λ_s^+ , we focus on a MANET with feedback and summarize in Fig. 7 how its throughput and delay vary with λ_s^+ and (B_s, B_r) . We can see from Fig. 7(a) and (c) that although in general we can improve T by increasing either B_s or B_r , the degree of such improvement is highly dependent on λ_s^+ . As λ_s^+ increases, the throughput improvement from B_r monotonically increases, while the corresponding improvement from B_s first increases and then decreases. Fig. 7(a) and (c) also show that as λ_s^+ increases, T under different settings of B_s finally converges to the same constant (i.e., T_c given by (17)), while T under a given setting of B_r converges to a distinct constant of T_c , which monotonically increases as B_r increases.

Regarding the joint impacts of λ_s^+ and B_s on delay performance, we can see clearly from Fig. 7(b) that just as discussed in Corollary 3, there exists a threshold of λ_s^+ beyond which $\mathbb{E}\{D\}$ will increase to infinity as B_s increases, while for a given λ_s^+ less than the threshold, $\mathbb{E}\{D\}$ almost keeps as a constant as B_s increases. About the joint impacts of λ_s^+ and B_r on delay performance, Fig. 7(d) shows that for a given setting of λ_s^+ , there also exists a threshold for B_r , beyond which $\mathbb{E}\{D\}$ almost keeps as a constant as B_r increases. It is interesting to see that such threshold for B_r and the corresponding delay constant tend to increase as λ_s^+ increases. The results in Fig. 7(d) imply that a bounded $\mathbb{E}\{D\}$ can be always guaranteed in a MANET as long as its source buffer size is limited.

Finally, we plot Fig. 8 to illustrate the network performance behaviors as the number of nodes n increases, where we set $B_s = 5$, $B_r = 5$, $\lambda_s^+ = 0.05$ and $d = 2$ (d denotes the node/cell density). We can see from Fig. 8(a) that for both the network scenarios without and with feedback, the per flow throughput T decreases monotonically as n increases. When n tends to infinity, from (24) and (25) we have p_{sd} and p_{sr} tend to 0 and $\frac{1-e^{-d}-de^{-d}}{2d}$, respectively, and from (17) we can further observe

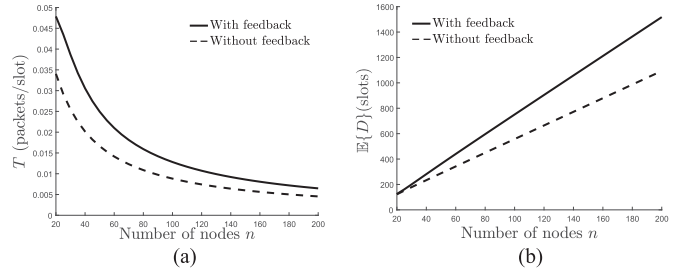


Fig. 8. Throughput and delay versus the number of nodes n for the network setting of $(B_s = 5, B_r = 5, \lambda_s^+ = 0.05, d = 2)$. (a) T versus n . (b) $\mathbb{E}\{D\}$ versus n .

that the throughput capacity scales as $\Theta(B_r/n)$. It indicates that to achieve a non-vanishing per flow throughput in a MANET under general limited buffer constraint, the relay buffer size B_r should grow at least linearly with the number of nodes n . Regarding the delay performance, Fig. 8(b) shows that for both the network scenarios without and with feedback, $\mathbb{E}\{D\}$ increases almost linearly with n . This linear growth behavior can be also observed in other works such as [9]–[11], while the new insight revealed here is that the cost of adopting feedback mechanism to improve throughput performance is a steeper growth slope of E2E delay with the network size.

VII. CONCLUSION

This paper explored, for the first time, the performance modeling for MANETs under the general limited buffer constraint. In particular, a complete and generally applicable theoretical framework was developed to capture the inherent buffer occupancy behaviors in such a MANET, which enables the exact expressions to be derived for some fundamental network performance metrics, like the achievable throughput, expected E2E delay and throughput capacity. Some interesting conclusions that can be drawn from this study are: 1) In general, adopting the feedback mechanism can lead to an improvement in the throughput performance, but such improvement comes with the cost of a relatively large delay; 2) For the purpose of throughput improvement, it is more efficient to adopt a large relay buffer rather than a large source buffer; 3) The throughput capacity is dominated by the relay buffer size rather than the source buffer size; 4) Feedback mechanism cannot improve the throughput capacity.

Notice that in this paper, only buffer constraint was investigated, so one promising future direction is to conduct performance study for MANETs under more practical network scenarios, where the packet loss could be caused by other reasons such as poor signal conditions. Another appealing future direction is to explore the performance modeling for MANETs with the retransmission scheme.

APPENDIX A PROOF OF LEMMA 1

Based on the transition scenarios, we can see $p_{i,i+1}$ is actually equal to the packet arrival rate λ_r^+ of the relay buffer, so we just need to determine λ_r^+ for the evaluation of $p_{i,i+1}$. When \mathcal{S} serves

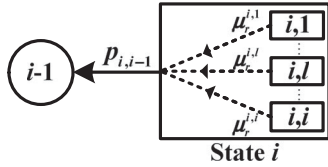


Fig. 9. Illustration of the state decomposition.

as a relay, all other $n - 2$ nodes (except \mathcal{S} and its destination \mathcal{D}) may forward packets to it. When one of these nodes sends out a packet from its source buffer, it will forward the packet to \mathcal{S} with probability $\frac{p_{sr}}{\mu_s(n-2)}$. This is because with probability $\frac{p_{sr}}{\mu_s}$ the packet is intended for a relay node, and each of the $n - 2$ relay nodes are equally likely. Thus,

$$p_{i,i+1} = \lambda_r^+ = (n-2)\lambda_s^- \cdot \frac{p_{sr}}{\mu_s(n-2)}, \quad (29)$$

where λ_s^- denotes the packet departure rate of a source buffer. Due to the reversibility of the B/B/1/ B_s queue, the packet departure process of the source buffer is also a Bernoulli process with its departure rate λ_s^- being determined as

$$\lambda_s^- = \mu_s (1 - \pi_s(0)). \quad (30)$$

Then we have

$$p_{i,i+1} = \lambda_r^+ = p_{sr} \cdot (1 - \pi_s(0)), \quad 0 \leq i \leq B_r - 1.$$

Regarding the evaluation of transition probability $p_{i,i-1}$, it is notable that $p_{i,i-1}$ just corresponds to the service rate μ_r^i of the relay buffer when it is at state i . To determine μ_r^i , we further decompose the state i ($i > 0$) into i sub-states $\{(i, l), 1 \leq l \leq i\}$ as illustrated in Fig. 9, where l denotes the number of non-empty relay queues in the relay buffer. Let $\mu_r^{i,l}$ denote the service rate of the relay buffer when it is at sub-state (i, l) , and let $P_{l|i}$ denote the probability that the relay buffer is at sub-state (i, l) conditioned on that the relay buffer is at state i , we then have

$$\mu_r^i = \sum_{l=1}^i P_{l|i} \cdot \mu_r^{i,l}. \quad (31)$$

We first derive the term $\mu_r^{i,l}$ in (31). Notice that with probability p_{rd} node \mathcal{S} conducts a Relay-to-Destination operation, and it will equally likely choose one of the $n - 2$ nodes (except \mathcal{S} and \mathcal{D}) as its receiver. Thus, when there are l non-empty relay queues in the relay buffer, the corresponding service rate $\mu_r^{i,l}$ is determined as

$$\mu_r^{i,l} = l \cdot \frac{p_{rd}}{n-2}. \quad (32)$$

To determine the conditional probability $P_{l|i}$, we adopt the following occupancy approach proposed in [31]. First, for the relay buffer with i packets, where each packet may be destined for any one of the $n - 2$ nodes (except \mathcal{S} and \mathcal{D}), the number of all possible cases N_i is

$$\binom{n-3+i}{i}.$$

Then, for the relay buffer with i packets, where these packets are destined for only l different nodes, the number of possible cases $N_{l|i}$ is

$$\binom{n-2}{l} \cdot \binom{(l-1) + (i-l)}{i-l}.$$

Finally, since the locations of nodes are independently and uniformly distributed, each case occurs with equal probability. According to the *Classical Probability*, we have

$$P_{l|i} = \frac{N_{l|i}}{N_i} = \frac{\binom{n-2}{l} \cdot \binom{i-l}{i-l}}{\binom{n-3+i}{i}}. \quad (33)$$

Substituting (32) and (33) into (31), $p_{i,i-1}$ is determined as

$$p_{i,i-1} = \mu_r^i = p_{rd} \cdot \frac{i}{n-3+i}, \quad 1 \leq i \leq B_r.$$

APPENDIX B

PROOF OF COROLLARY 1

For the network scenario with feedback, although node \mathcal{S} gets the chance to execute the Source-to-Relay operation in a time slot, it still remains idle if the relay buffer of its intended receiver is full (with the overflow probability $\pi_r(B_r)$). Thus, the service rate μ_s of source buffer of node \mathcal{S} is given by

$$\mu_s = p_{sd} + p_{sr} \cdot (1 - \pi_r(B_r)).$$

Based on the similar analysis as that in Section III-A, the OSD Π_s of source buffer here can also be determined by expression (3), and the one-step transition probabilities of the birth-death chain of relay buffer can be determined as

$$\begin{aligned} p_{i,i+1} &= \lambda_r^+, \\ p_{i,i-1} &= p_{rd} \cdot \frac{i}{n-3+i}, \end{aligned}$$

where λ_r^+ denotes the packet arrival rate of the relay buffer when the relay buffer is not full. Regarding the evaluation of λ_r^+ , we have

$$\begin{aligned} &\lambda_r^+ \cdot (1 - \pi_r(B_r)) + 0 \cdot \pi_r(B_r) \\ &= (n-2)\lambda_s^- \cdot \frac{p_{sr}(1 - \pi_r(B_r))}{\mu_s(n-2)}, \end{aligned} \quad (34)$$

$$\Rightarrow \lambda_r^+ = \lambda_s^- \frac{p_{sr}}{\mu_s} = p_{sr} \cdot (1 - \pi_s(0)), \quad (35)$$

where λ_s^- denotes the packet departure rate of a source buffer, and (35) follows from (30). Notice that the transition probabilities here are the same as that under the scenario without feedback, thus the OSD Π_r of the relay buffer here can also be determined by expression (9).

APPENDIX C

FIXED POINT ITERATION FOR SOLVING $\pi_r(B_r)$

Since $\pi_r(B_r)$ is the fixed point of equation (11), we apply the fixed point iteration to solve $\pi_r(B_r)$. The detailed algorithm of

Algorithm 1: Fixed Point Iteration.**Require:**

Basic network parameters $\{n, B_s, B_r, \lambda_s^+, p_{sd}, p_{sr}, p_{rd}\}$;

Ensure:

Relay buffer overflow probability $\pi_r(B_r)$;

- 1: Set $x_1 = 0$ and $i = 1$;
- 2: **while** $(x_i - x_{i-1} \geq \delta) \vee (i = 1)$ **do**
- 3: $i = i + 1$;
- 4: $\mu_s = p_{sd} + p_{sr} \cdot (1 - x_{i-1})$;
- 5: $\tau = \frac{\lambda_s^+(1-\mu_s)}{\mu_s(1-\lambda_s^+)}$;
- 6: $\pi_s(0) = \frac{\mu_s - \lambda_s^+}{\mu_s - \lambda_s^+ \cdot \tau^{B_s}}$;
- 7: $x_i = \frac{C_{B_r}(1-\pi_s(0))^{B_r}}{\sum_{k=0}^{B_r} C_k(1-\pi_s(0))^k}$;
- 8: **end while**
- 9: $\pi_r(B_r) = x_i$;
- 10: **return** $\pi_r(B_r)$;

the fixed point iteration is summarized in Algorithm 1, where δ represents the accuracy can be achieved by the algorithm.⁴

APPENDIX D
PROOF OF THEOREM 1

Let T_1 and T_2 denote the packet delivery rates at the destination of node \mathcal{S} through the one-hop transmission and the two-hop transmission respectively, then we have

$$T_1 = \lambda_s^- \cdot \frac{p_{sd}}{\mu_s}, \quad (36)$$

$$T_2 = \lambda_s^- \cdot \frac{p_{sr}(1 - \pi_r(B_r))}{\mu_s}, \quad (37)$$

where λ_s^- denotes the packet departure rate of source buffer of \mathcal{S} . Substituting (30) into (36) and (37), then (13) follows from $T = T_1 + T_2$.

Regarding the expected E2E delay $\mathbb{E}\{D\}$, we focus on a tagged packet p of node \mathcal{S} and evaluate its expected source queuing delay $\mathbb{E}\{D_{S_Q}\}$ and expected delivery delay $\mathbb{E}\{D_D\}$, respectively. For the evaluation of $\mathbb{E}\{D_{S_Q}\}$ we have

$$\mathbb{E}\{D_{S_Q}\} = \frac{L_s}{\mu_s}. \quad (38)$$

Let $\pi_s^*(i)$ ($0 \leq i \leq B_s - 1$) denote the probability that there are i packets in the source buffer conditioned on that the source buffer is not full, then $\pi_s^*(i)$ is determined as [21]

$$\pi_s^*(i) = \frac{\lambda_s^+}{(1 - \lambda_s^+)^2} \tau^i \cdot H_1^{-1}, \quad 0 \leq i \leq B_r - 1$$

where H_1 is the normalization constant. Since $\sum_{i=1}^{B_s-1} \pi_s^*(i) = 1$, we have

$$\pi_s^*(i) = \frac{1 - \tau}{1 - \tau^{B_s}} \tau^i, \quad 0 \leq i \leq B_r - 1.$$

⁴The smaller δ is, the higher accuracy can be achieved, coming with a cost of more iterations. In our experiment, we set δ to be 10^{-6} to achieve a high accuracy. The execution time of the algorithm under this setting is usually less than 0.2 seconds.

Then L_s is given by

$$L_s = \sum_{i=0}^{B_s-1} i \pi_s^*(i) = \frac{\tau - B_s \tau^{B_s} + (B_s - 1) \tau^{B_s+1}}{(1 - \tau)(1 - \tau^{B_s})}.$$

After moving to the HoL in its source buffer, packet p will be sent out by node \mathcal{S} with mean service time $1/\mu_s$, and it may be delivered to its destination directly or forwarded to a relay. Let $\mathbb{E}\{D_R\}$ denote the expected time that p takes to reach its destination after it is forwarded to a relay, then we have

$$\mathbb{E}\{D_D\} = \frac{1}{\mu_s} + \frac{T_1}{T_1 + T_2} \cdot 0 + \frac{T_2}{T_1 + T_2} \cdot \mathbb{E}\{D_R\}. \quad (39)$$

Based on the OSD Π_r , L_r is given by (16). Due to the symmetry of relay queues in a relay buffer, the mean number of packets in one relay queue is $L_r/(n-2)$, and the service rate of each relay queue is $p_{rd}/(n-2)$. Thus, $\mathbb{E}\{D_R\}$ can be determined as

$$\mathbb{E}\{D_R\} = \left(\frac{L_r}{n-2} + 1 \right) \cdot \left(\frac{p_{rd}}{n-2} \right)^{-1}. \quad (40)$$

Substituting (40) into (39), then (14) follows from $\mathbb{E}\{D\} = \mathbb{E}\{D_{S_Q}\} + \mathbb{E}\{D_D\}$.

APPENDIX E
PROOF OF COROLLARY 2

From expressions (1) and (10), we can see that the for a given packet generating rate λ_s^+ , the service rate μ_s of the source buffer under the scenario with feedback is smaller than that under the scenario without feedback. From (3) we have

$$\begin{aligned} \frac{\partial \pi_s(0)}{\partial \mu_s} &= \frac{\mu_s - \lambda_s^+ \tau^{B_s} - \left(1 - \lambda_s^+ B_s \tau^{B_s-1} \frac{\partial \tau}{\partial \mu_s}\right) (\mu_s - \lambda_s^+)}{(\mu_s - \lambda_s^+ \tau^{B_s})^2} \\ &= \frac{\lambda_s^+ - \lambda_s^+ \tau^{B_s} - B_s \frac{\lambda_s^+ (\mu_s - \lambda_s^+)}{\mu_s (1 - \mu_s)} \tau^{B_s}}{(\mu_s - \lambda_s^+ \tau^{B_s})^2} \\ &= \frac{\lambda_s^+ (\mu_s - \lambda_s^+)^2}{(\mu_s - \lambda_s^+ \tau^{B_s})^2 \cdot \mu_s^2 \cdot (1 - \lambda_s^+)} \cdot \sum_{i=0}^{B_s-1} \left(1 + \frac{i}{1 - \mu_s}\right) \tau^i \\ &> 0, \end{aligned} \quad (41)$$

which indicates that $\pi_s(0)$ under the scenario with feedback is smaller than that under the scenario without feedback.

We let $r = \frac{1}{1 - \pi_s(0)}$ and substitute r into (13), then T can be expressed as

$$T = p_{sd} \cdot \frac{1}{r} + p_{sr} \cdot \frac{1}{g(r)}, \quad (42)$$

where $g(r) = r \cdot \left(1 + \frac{C_{B_r}}{h(r)}\right)$ and $h(r) = \sum_{i=0}^{B_r-1} C_i r^{B_r-i}$. Regarding the derivative of $g(r)$ we have

$$g'(r) = \frac{1}{h(r)^2} \underbrace{\{h(r)(h(r) + C_{B_r}) - r C_{B_r} h'(r)\}}_{(a)}, \quad (43)$$

where

$$\begin{aligned}
(a) &= \sum_{i=0}^{B_r-1} C_i r^{B_r-i} \cdot \sum_{i=0}^{B_r-1} C_i r^{B_r-i} \\
&\quad - C_{B_r} \sum_{i=0}^{B_r-1} (B_r - i) C_i r^{B_r-i} \\
&= \sum_{i=1}^{B_r} C_{B_r-i} r^i \cdot \sum_{i=0}^{B_r} C_{B_r-i} r^i - \sum_{i=1}^{B_r} i C_{B_r} C_{B_r-i} r^i \\
&= \sum_{i=1}^{B_r} \left(\sum_{j=0}^{i-1} C_{B_r-j} r^j C_{B_r-i+j} r^{i-j} - i C_{B_r} C_{B_r-i} r^i \right) \\
&\quad + \sum_{i=B_r+1}^{2B_r} \sum_{j=i-B_r}^{B_r} C_{B_r-j} r^j C_{B_r-i+j} r^{i-j} \\
&> \sum_{i=1}^{B_r} \left(\sum_{j=0}^{i-1} C_{B_r-j} C_{B_r-i+j} - i C_{B_r} C_{B_r-i} \right) r^i > 0,
\end{aligned} \tag{44}$$

here (44) is because that $C_{B_r-j} C_{B_r-i+j} > C_{B_r} C_{B_r-i}$ for $0 < j < i$.

We can see from (41) that $\pi_s(0)$ increases as μ_s increases, and from (42)–(44) that T increases as $\pi_s(0)$ decreases. Thus, we can conclude that T under the scenario with feedback is larger than that under the scenario without feedback, which indicates that adopting the feedback mechanism improves the throughput performance.

APPENDIX F PROOF OF LEMMA 2

For the scenario without feedback, we know from (3) that

$$\begin{aligned}
\frac{\partial \pi_s(0)}{\partial \lambda_s^+} &= \frac{-\mu_s + \lambda_s^+ \tau^{B_s} + \left(\tau^{B_s} + \lambda_s^+ B_s \tau^{B_s-1} \frac{\partial \tau}{\partial \lambda_s^+} \right) (\mu_s - \lambda_s^+)}{(\mu_s - \lambda_s^+ \tau^{B_s})^2} \\
&= \frac{-\mu_s + \mu_s \tau^{B_s} + B_s \frac{\mu_s - \lambda_s^+}{1 - \lambda_s^+} \tau^{B_s}}{(\mu_s - \lambda_s^+ \tau^{B_s})^2} \\
&= \frac{-(\lambda_s^+ - \mu_s)^2}{(\mu_s - \lambda_s^+ \tau^{B_s})^2 \cdot (1 - \lambda_s^+)^2 \cdot \mu_s} \cdot \sum_{i=1}^{B_s} i \tau^{i-1} < 0.
\end{aligned} \tag{45}$$

Thus, as λ_s^+ increases, $\pi_s(0)$ decreases which leads to an increase in T (refer to the analysis in Appendix E).

For the scenario with feedback, as λ_s^+ increases, the MANET tends to be more congested with a larger $\pi_r(B_r)$. Thus, we know from (10) that the corresponding μ_s decreases, and then from (41) that $\pi_s(0)$ decreases, leading to an increase in T .

APPENDIX G PROOF OF COROLLARY 3

From an intuitive point of view, a larger buffer implies that more packets can be stored and packet loss can be reduced, thus

a higher throughput can be achieved. More formally, from (3) we have

$$\begin{aligned}
&\pi_s(0)|_{B_s=K+1} - \pi_s(0)|_{B_s=K} \\
&= \frac{\lambda_s^+ \tau^K (\mu_s - \lambda_s^+) (\tau - 1)}{(\mu_s - \lambda_s^+ \tau^{K+1}) (\mu_s - \lambda_s^+ \tau^K)} < 0,
\end{aligned} \tag{46}$$

where (46) follows since $\tau > 1$ when $\lambda_s^+ > \mu_s$ and $\tau < 1$ when $\lambda_s^+ < \mu_s$. Then we can conclude that as B_s increases, $\pi_s(0)$ decreases, leading to an increase in T .

Let $r = \frac{1}{1 - \pi_s(0)}$ and substitute r into (9), then we have

$$\begin{aligned}
&\pi_r(B_r)|_{B_r=K+1} - \pi_r(B_r)|_{B_r=K} \\
&= \frac{C_{K+1} r^{-K-1}}{\sum_{i=0}^{K+1} C_i r^{-i}} - \frac{C_K r^{-K}}{\sum_{i=0}^K C_i r^{-i}} \\
&= \frac{C_{K+1} r^{-K-1} \sum_{i=0}^K C_i r^{-i} - C_K r^{-K} \sum_{i=0}^{K+1} C_i r^{-i}}{\sum_{i=0}^{K+1} C_i r^{-i} \cdot \sum_{i=0}^K C_i r^{-i}},
\end{aligned}$$

where

$$\begin{aligned}
(b) &= C_{K+1} r^{-K-1} \sum_{i=0}^K C_i r^{-i} - C_K r^{-K} \sum_{i=1}^{K+1} C_i r^{-i} - C_K r^{-K} \\
&< \sum_{i=0}^K (C_{K+1} C_i - C_K C_{i+1}) r^{-k-i-1} < 0.
\end{aligned}$$

Then we can conclude that as B_r increases, $\pi_r(B_r)$ decreases, leading to an increase in T (refer to expression (13)).

Regarding the infinite source buffer (i.e., $B_s \rightarrow \infty$), $\tau \geq 1$ when $\lambda_s^+ \geq \mu_s$, and we have

$$\begin{aligned}
\lim_{B_s \rightarrow \infty} \pi_s(0) &= \lim_{B_s \rightarrow \infty} \frac{\mu_s - \lambda_s^+}{\mu_s - \lambda_s^+ \tau^{B_s}} = 0, \\
\lim_{B_s \rightarrow \infty} T &= p_{sd} + p_{sr} \cdot \frac{\sum_{k=1}^{B_r} C_{k-1}}{\sum_{k=0}^{B_r} C_k} \\
&= p_{sd} + p_{sr} \frac{B_r}{n - 2 + B_r} = T_c.
\end{aligned}$$

According to the Queuing theory [21], for a Bernoulli/Bernoulli queue (i.e., the buffer size is infinite), its queue length tends to infinity when the corresponding arrival rate is equal to or larger than the service rate. Thus, we have $L_s \rightarrow \infty$, which leads that $\mathbb{E}\{D_{S_Q}\} \rightarrow \infty$ and $\mathbb{E}\{D\} \rightarrow \infty$.

When $\lambda_s^+ < \mu_s$, $\tau < 1$, and we have

$$\begin{aligned}
\lim_{B_s \rightarrow \infty} \pi_s(0) &= \lim_{B_s \rightarrow \infty} \frac{\mu_s - \lambda_s^+}{\mu_s - \lambda_s^+ \tau^{B_s}} = 1 - \frac{\lambda_s^+}{\mu_s}, \\
\lim_{B_s \rightarrow \infty} T &= p_{sd} \cdot \frac{\lambda_s^+}{\mu_s} + p_{sr} \cdot \frac{\sum_{k=0}^{B_r-1} C_k \left(\frac{\lambda_s^+}{\mu_s}\right)^{k+1}}{\sum_{k=0}^{B_r} C_k \left(\frac{\lambda_s^+}{\mu_s}\right)^k}.
\end{aligned}$$

Based on the analysis in Appendix D, L_s is determined as

$$\lim_{B_s \rightarrow \infty} L_s = \lim_{B_s \rightarrow \infty} \frac{1 - \tau}{1 - \tau^{B_s}} \sum_{i=0}^{B_s-1} i \tau^i = \frac{\tau}{1 - \tau}. \tag{47}$$

Substituting (47) into (14) we obtain (23b).

Regarding the infinite relay buffer (i.e., $B_r \rightarrow \infty$), from (9) and (16) we have

$$\lim_{B_r \rightarrow \infty} \pi_r(B_r) = \lim_{B_r \rightarrow \infty} C_{B_r} (1 - \pi_s(0))^{B_r} \cdot \pi_s(0)^{n-2} \quad (48)$$

$$\begin{aligned} &\leq \lim_{B_r \rightarrow \infty} (B_r + n)^n (1 - \pi_s(0))^{B_r} \\ &\leq \lim_{B_r \rightarrow \infty} 2^n B_r^n (1 - \pi_s(0))^{B_r} \\ &= \lim_{B_r \rightarrow \infty} \frac{2^n n! (1 - \pi_s(0))^{B_r}}{(\ln \frac{1}{1 - \pi_s(0)})^n} = 0, \end{aligned} \quad (49)$$

$$\begin{aligned} \lim_{B_r \rightarrow \infty} L_r &= \frac{\sum_{k \geq 0} k C_k (1 - \pi_s(0))^k}{\sum_{k \geq 0} C_k (1 - \pi_s(0))^k} \\ &= \frac{-(1 - \pi_s(0)) \cdot (\sum_{k \geq 0} C_k (1 - \pi_s(0))^k)'}{\sum_{k \geq 0} C_k (1 - \pi_s(0))^k} \\ &= -(1 - \pi_s(0)) \cdot (\pi_s(0)^{2-n})' \cdot \pi_s(0)^{n-2} \quad (50) \\ &= \frac{(n-2)(1 - \pi_s(0))}{\pi_s(0)}, \end{aligned} \quad (51)$$

where (48) and (50) follow since $\sum_{k \geq 0} C_k (1 - \pi_s(0))^k$ is just the Taylor-series expansion [32] of $\pi_s(0)^{2-n}$, and (49) follows from the L'Hôpital's rule [32]. Substituting (49) into (13) we obtain (22b), and substituting (49) and (51) into (14) we obtain (23c).

Regarding the MANET without buffer constraint (i.e., $B_s \rightarrow \infty$ and $B_r \rightarrow \infty$), we can directly obtain (22c) and (23d) by combining the corresponding results of the infinite source buffer scenario and the infinite relay buffer scenario.

APPENDIX H

DERIVATIONS OF PROBABILITIES p_{sd} , p_{sr} AND p_{rd}

For a cell-partitioned MANET with LS-MAC, the event that node \mathcal{S} gets the chance to execute the Source-to-Destination (resp. Source-to-Relay or Relay-to-Destination) operation in a time slot can be divided into the following sub-events: (1) its destination is (resp. is not) in the same cell with \mathcal{S} ; (2) other k out of $n-2$ nodes are in the same cell with \mathcal{S} , while the remaining $n-2-k$ nodes are not in this cell; (3) \mathcal{S} contends for the wireless channel access successfully. Thus we have

$$\begin{aligned} p_{sd} &= \sum_{k=0}^{n-2} \binom{n-2}{k} \left(\frac{1}{m^2}\right)^{k+1} \left(1 - \frac{1}{m^2}\right)^{n-2-k} \cdot \frac{1}{k+2} \\ &= \sum_{k=0}^{n-2} \binom{n-1}{k+1} \left(\frac{1}{m^2}\right)^{k+1} \left(1 - \frac{1}{m^2}\right)^{n-2-k} \cdot \frac{1}{k+2} \\ &\quad - \sum_{k=0}^{n-3} \binom{n-2}{k+1} \left(\frac{1}{m^2}\right)^{k+1} \left(1 - \frac{1}{m^2}\right)^{n-2-k} \cdot \frac{1}{k+2} \\ &= \frac{m^2}{n} \left\{ 1 - \left(1 - \frac{1}{m^2}\right)^n \right\} - \left(1 - \frac{1}{m^2}\right)^{n-1} \end{aligned}$$

$$\begin{aligned} &- \frac{m^2 - 1}{n-1} \left\{ 1 - \left(1 - \frac{1}{m^2}\right)^{n-1} \right\} + \left(1 - \frac{1}{m^2}\right)^{n-1} \\ &= \frac{m^2}{n} - \frac{m^2 - 1}{n-1} + \left(\frac{m^2 - 1}{n-1} - \frac{m^2 - 1}{n}\right) \left(1 - \frac{1}{m^2}\right)^{n-1}, \end{aligned}$$

and

$$\begin{aligned} p_{sr} &= p_{rd} \\ &= \frac{1}{2} \sum_{k=1}^{n-2} \binom{n-2}{k} \left(\frac{1}{m^2}\right)^k \left(1 - \frac{1}{m^2}\right)^{n-1-k} \cdot \frac{1}{k+1} \\ &= \frac{1}{2} \left\{ \frac{m^2 - 1}{n-1} - \frac{m^2}{n-1} \left(1 - \frac{1}{m^2}\right)^n - \left(1 - \frac{1}{m^2}\right)^{n-1} \right\}. \end{aligned}$$

For a cell-partitioned MANET with EC-MAC, by applying the similar approach and algebraic operations we have

$$\begin{aligned} p_{sd} &= \frac{1}{\varepsilon^2} \left\{ \sum_{k=0}^{n-2} \binom{n-2}{k} \left(\frac{1}{m^2}\right)^{k+1} \left(1 - \frac{1}{m^2}\right)^{n-2-k} \cdot \frac{1}{k+2} \right. \\ &\quad \left. + \sum_{k=0}^{n-2} \binom{n-2}{k} \left(\frac{1}{m^2}\right)^{k+1} \left(1 - \frac{1}{m^2}\right)^{n-2-k} \cdot \frac{4v^2 - 4v}{k+1} \right\} \\ &= \frac{1}{\varepsilon^2} \left\{ \frac{\Gamma - \frac{m^2}{n}}{n-1} + \frac{m^2 - 1 - (\Gamma - 1)n}{n(n-1)} \left(1 - \frac{1}{m^2}\right)^{n-1} \right\}, \end{aligned}$$

and

$$\begin{aligned} p_{sr} &= p_{rd} \\ &= \frac{1}{2\varepsilon^2} \frac{m^2 - \Gamma}{m^2} \\ &\quad \left\{ \sum_{k=1}^{n-2} \binom{n-2}{k} \left(\frac{1}{m^2}\right)^k \left(1 - \frac{1}{m^2}\right)^{n-2-k} \cdot \frac{1}{k+1} \right. \\ &\quad \left. + \sum_{k=1}^{n-2} \binom{n-2}{k} \left(\frac{\Gamma - 1}{m^2}\right)^k \left(\frac{m^2 - \Gamma}{m^2}\right)^{n-2-k} \right\} \\ &= \frac{1}{2\varepsilon^2} \left\{ \frac{m^2 - \Gamma}{n-1} \left(1 - \left(1 - \frac{1}{m^2}\right)^{n-1}\right) - \left(1 - \frac{\Gamma}{m^2}\right)^{n-1} \right\}. \end{aligned}$$

REFERENCES

- [1] R. Ramanathan and J. Redi, "A brief overview of ad hoc networks: Challenges and directions," *IEEE Commun. Mag.*, vol. 40, no. 5, pp. 20–22, May 2002.
- [2] M. N. Tehrani, M. Uysal, and H. Yanikomeroglu, "Device-to-device communication in 5g cellular networks: challenges, solutions, and future directions," *IEEE Commun. Mag.*, vol. 52, no. 5, pp. 86–92, May 2014.
- [3] H. Shariatmadari *et al.*, "Machine-type communications: Current status and future perspectives toward 5g systems," *IEEE Commun. Mag.*, vol. 53, no. 9, pp. 10–17, Sep. 2015.
- [4] H. Hartenstein and L. Laberteaux, "A tutorial survey on vehicular ad hoc networks," *IEEE Commun. Mag.*, vol. 46, no. 6, pp. 164–171, Jun. 2008.
- [5] Z. Luo, X. Gan, X. Wang, and H. Luo, "Optimal throughput–delay tradeoff in manets with supportive infrastructure using random linear coding," *IEEE Trans. Veh. Technol.*, vol. 65, no. 9, pp. 7543–7558, Sep. 2016.
- [6] J. Andrews *et al.*, "Rethinking information theory for mobile ad hoc networks," *IEEE Commun. Mag.*, vol. 46, no. 12, pp. 94–101, Dec. 2008.

- [7] A. Goldsmith, M. Effros, R. Koetter, M. Medard, and L. Zheng, "Beyond Shannon: The quest for fundamental performance limits of wireless ad hoc networks," *IEEE Commun. Mag.*, vol. 49, no. 5, pp. 195–205, May 2011.
- [8] M. Grossglauser and D. Tse, "Mobility increases the capacity of ad hoc wireless networks," *IEEE/ACM Trans. Netw.*, vol. 10, no. 4, pp. 477–486, Aug. 2002.
- [9] M. J. Neely and E. Modiano, "Capacity and delay tradeoffs for ad-hoc mobile networks," *IEEE Trans. Inf. Theory*, vol. 51, no. 6, pp. 1917–1936, Jun. 2005.
- [10] A. E. Gamal, J. Mammen, B. Prabhakar, and D. Shah, "Optimal throughput-delay scaling in wireless networks—Part I: The fluid model," *IEEE Trans. Inf. Theory*, vol. 52, no. 6, pp. 2568–2592, Jun. 2006.
- [11] G. Sharma, R. R. Mazumdar, and N. B. Shroff, "Delay and capacity tradeoffs in mobile ad hoc networks: A global perspective," *IEEE/ACM Trans. Netw.*, vol. 15, no. 5, pp. 981–992, Oct. 2007.
- [12] X. Wang, W. Huang, S. Wang, J. Zhang, and C. Hu, "Delay and capacity tradeoff analysis for motioncast," *IEEE/ACM Trans. Netw.*, vol. 19, no. 5, pp. 1354–1367, Oct. 2011.
- [13] Y. Wang, X. Chu, X. Wang, and Y. Cheng, "Optimal multicast capacity and delay tradeoffs in manets: A global perspective," in *Proc. IEEE INFOCOM*, 2011, pp. 640–648.
- [14] Y. Qin, X. Tian, W. Wu, and X. Wang, "Mobility weakens the distinction between multicast and unicast," *IEEE/ACM Trans. Netw.*, vol. 24, no. 3, pp. 1350–1363, Jun. 2016.
- [15] J. D. Herdtnr and E. K. Chong, "Throughput-storage tradeoff in ad hoc networks," in *Proc. IEEE INFOCOM*, 2005, pp. 2536–2542.
- [16] J. Gao, Y. Shen, X. Jiang, and J. Li, "Source delay in mobile ad hoc networks," *Ad Hoc Networks*, vol. 24, pp. 109–120, 2015.
- [17] J. Liu, M. Sheng, Y. Xu, J. Li, and X. Jiang, "End-to-end delay modeling in buffer-limited manets: A general theoretical framework," *IEEE Trans. Wireless Commun.*, vol. 15, no. 1, pp. 498–511, Jan. 2016.
- [18] J. Liu, M. Sheng, Y. Xu, J. Li, and X. Jiang, "On throughput capacity for a class of buffer-limited manets," *Ad Hoc Networks*, vol. 37, pp. 354–367, 2016.
- [19] P. Nain, D. Towsley, B. Liu, and Z. Liu, "Properties of random direction models," in *Proc. IEEE INFOCOM*, 2005, pp. 1897–1907.
- [20] T. G. Robertazzi, *Computer Networks and Systems: Queueing Theory and Performance Evaluation*. New York, NY, USA: Springer Science & Business Media, 2012.
- [21] H. Daduna, *Queueing Networks with Discrete Time Scale: Explicit Expressions for the Steady State Behavior of Discrete Time Stochastic Networks*. New York, NY, USA: Springer-Verlag, 2001.
- [22] A. Granas and J. Dugundji, *Fixed Point Theory*. New York, NY, USA: Springer-Verlag, 2003.
- [23] R. Urgaonkar and M. J. Neely, "Network capacity region and minimum energy function for a delay-tolerant mobile ad hoc network," *IEEE/ACM Trans. Netw.*, vol. 19, no. 4, pp. 1137–1150, Aug. 2011.
- [24] S. R. Kulkarni and P. Viswanath, "A deterministic approach to throughput scaling in wireless networks," *IEEE Trans. Inf. Theory*, vol. 50, no. 6, pp. 1041–1049, Jun. 2004.
- [25] M. Franceschetti, O. Dousse, D. N. Tse, and P. Thira, "Closing the gap in the capacity of wireless networks via percolation theory," *IEEE Trans. Inf. Theory*, vol. 53, no. 3, pp. 1009–1018, Mar. 2007.
- [26] S. Shakkottai, X. Liu, and R. Srikant, "The multicast capacity of large multihop wireless networks," *IEEE/ACM Trans. Netw.*, vol. 18, no. 6, pp. 1691–1700, Dec. 2010.
- [27] P. Gupta and P. Kumar, "The capacity of wireless networks," *IEEE Trans. Inf. Theory*, vol. 46, no. 2, pp. 388–404, Mar. 2000.
- [28] Y. Chen, Y. Shen, J. Zhu, X. Jiang, and H. Tokuda, "On the throughput capacity study for aloha mobile ad hoc networks," *IEEE Trans. Commun.*, vol. 64, no. 4, pp. 1646–1659, Apr. 2016.
- [29] J. Liu and Y. Xu, "C++ simulator: Performance modeling for manets under general limited buffer constraint," 2015. [Online]. Available: https://www.researchgate.net/profile/Jia_Liu100, DOI: 10.13140/RG.2.1.1266.8248.
- [30] S. McCanne and S. Floyd, "Network simulator ns-2," 1997. [Online]. Available: <http://www.isi.edu/nsnam/ns/>
- [31] H. Stark and J. W. Woods, *Probability and Random Processes With Applications to Signal Processing*. Englewood Cliffs, NJ, USA: Prentice-Hall, 2002.
- [32] J. Stewart, *Calculus*. Boston, MA, USA: Cengage Learning, 2011.



Jia Liu (S'16–M'17) received the Ph.D. degree from the School of Systems Information Science, Future University Hakodate, Hakodate, Japan, in 2016. He is currently an Assistant Professor in the Center for Cybersecurity Research and Development, National Institute of Informatics, Japan. His research interests include mobile ad hoc networks, 5G communication systems, D2D communications, cyber security, etc. He has published about 15 technical papers at premium international journals and conferences, like IEEE TRANSACTIONS ON WIRELESS COMMUNICATION, *Computer Networks*, *Ad Hoc Networks*, *Computer Communications*, IEEE ICC, and IEEE WCNC.



Yang Xu (M'16) received the B.E. degree in communications engineering and the Ph.D. degree in communication and information systems from Xidian University, Xi'an, China, in 2006 and 2014, respectively. She is currently a Lecturer at the School of Economics and Management, Xidian University, and also a Visiting Scholar in Future University Hakodate. She has published about 15 papers at premium international journals and conferences, including IEEE TRANSACTIONS ON WIRELESS COMMUNICATION, *Computer Networks*, *Ad Hoc Networks*, *Wireless Networks*, IEEE ICC, and IEEE WCNC. Her current research interests include physical-layer security, blockchain and wireless communications.



Yulong Shen received the B.S. and M.S. degrees in computer science and the Ph.D. degree in cryptography from Xidian University, Xian, China, in 2002, 2005, and 2008, respectively. He is currently a Professor at the School of Computer Science and Technology, Xidian University, China. He is also an Associate Director of the Shaanxi Key Laboratory of Network and System Security and a member of the State Key Laboratory of Integrated Services Networks Xidian University, China. He has also served on the technical program committees of several international conferences, including ICEBE, INCoS, CIS, and SOWN. His research interests include Wireless network security and cloud computing security.



Xiaohong Jiang received the B.S., M.S., and Ph.D. degrees in 1989, 1992, and 1999 respectively, all from Xidian University, Xi'an, China. He is currently a Full Professor of Future University Hakodate, Japan. Before joining Future University, he was an Associate professor, Tohoku University, from February 2005 to March 2010. His research interests include computer communications networks, mainly wireless networks and optical networks, network security, routers/switches design, etc. He has published more than 260 technical papers at premium international journals and conferences, which include more than 50 papers published in top IEEE journals and top IEEE conferences, like IEEE/ACM TRANSACTIONS ON NETWORKING, IEEE JOURNAL OF SELECTED AREAS ON COMMUNICATIONS, IEEE TRANSACTIONS ON PARALLEL AND DISTRIBUTED SYSTEMS, IEEE INFOCOM. He received the Best Paper Award of IEEE HPCC 2014, IEEE WCNC 2012, IEEE WCNC 2008, IEEE ICC 2005-Optical Networking Symposium, and IEEE/IEICE HPSR 2002. He is a Member of ACM and IEICE.



Tarik Taleb (S'04–M'05–SM'10) received the B.E. degree in information engineering and the M.Sc. and Ph.D. degrees in information sciences from Tohoku University, Sendai, Japan, in 2001, 2003, and 2005, respectively. He was an Assistant Professor with the Graduate School of Information Sciences, Tohoku University, Sendai, Japan. He has been a Senior Researcher and 3GPP Standardization Expert with NEC Europe Ltd., Heidelberg, Germany. He is currently a Professor with the School of Electrical Engineering, Aalto University. His current research interests include architectural enhancements to mobile core networks, mobile cloud networking, mobile multimedia streaming, and social media networking. He has also been directly involved in the development and standardization of the evolved packet system as a member of 3GPP's System Architecture Working Group. He has received many awards, including the IEEE ComSoc Asia Pacific Best Young Researcher Award in 2009, and some of his research work has also received best paper awards at prestigious conferences.